

Fracture Toughness Properties of High-Strength Martensitic Steel within a Wide Hardness Range

N.M. Abd-Allah, M.S. El-Fadaly, M.M. Megahed, and A.M. Eleiche

(Submitted 5 February 2001; in revised form 17 May 2001)

Fracture toughness tests were carried out on six grades of high-strength martensitic steel within the hardness range from 270 to 475 HB. Four types of tests were performed: (a) Charpy V-notch (CVN) impact over the temperature range -120 to 60 °C, (b) plane strain fracture toughness, K_{IC} , near the onset of crack growth, (c) fracture toughness, J_{IC} , near the initiation of slow crack growth, and (d) fracture toughness, J_{IC} , and crack tip opening displacement (CTOD_{IC}) at the onset of slow crack growth using direct current potential drop (DCPD) technique. Further, true plane strain fracture toughness, K_o , at the onset of crack initiation was determined. Fracture toughness behavior including the measured and determined values of CVN, K_{IC} , K_o , J_{IC} , J_{IC} , and CTOD_{IC} have been interrelated over the entire hardness range using the various analytical and empirical correlations reported in the literature. The results indicate that the steel acquires the optimum fracture toughness properties at a hardness of 305 HB, corresponding to a tempering temperature of 630 °C. Further, the steel exhibits a slight 300 °C temper embrittlement phenomenon.

Keywords Charpy V-notch, crack tip opening displacement, direct current potential drop, plane strain fracture toughness, stress intensity factor, temper embrittlement, transition temperature, true plane fracture toughness

1. Introduction

Prior to the development of fracture mechanics, the Charpy V-notch (CVN) impact test was the one most widely used to determine the fracture toughness behavior of structural materials. There are some valid criticisms of this test, when compared with fracture toughness K_{IC} and J_{IC} tests, such as the small specimen size, the presence of a blunt notch with root radius of 0.25 mm, and the inability to differentiate between initiation and propagation energies. Nevertheless, this test is still popular today because it is simple, fast, and inexpensive. Furthermore, there exist in the literature many generally accepted correlations between the CVN impact and the K_{IC} tests.^[1]

The behavior exhibited by the tested material, whether brittle or ductile, depends on whether the normal stress exceeds the cohesive strength before the shear stress exceeds the material shear strength. It follows that brittle fracture is promoted by increasing the triaxiality factor (η), increasing the speed of deformation (ϵ), and decreasing the temperature (T). On the other hand, ductile fracture will dominate with decreasing η , decreasing ϵ , and increasing temperature T .^[2] By keeping η and ϵ the same during CVN impact testing, most metals exhibit

four broad ranges of fracture through their transition-temperature response. These four ranges are the lower shelf of material linear-elastic behavior, lower transition of material elasto-plastic behavior with no stable crack growth prior to brittle fracture, upper transition of stable ductile tearing followed by brittle fracture, and upper shelf of full fibrous ductile tearing.^[3]

Linear elastic fracture mechanics (LEFM) is established for materials that fracture when crack-tip plasticity ahead of the crack tip is sufficiently small to be within the singularity dominated zone. However, for materials that show a significant amount of plasticity before the onset of stable crack growth, the LEFM concept is no longer applicable or practicable. Under such conditions, elastic-plastic fracture mechanics parameters, such as J -integral and crack-tip opening displacement (CTOD), are used to characterize the fracture behavior of ductile materials. Besides critical values of J (J_{IC}) and J -crack growth resistance curves, J -initiation (J_{IC}) and CTOD-initiation (CTOD_{IC}) values are the basic criteria for the characterization of fracture resistance of materials used in the transition and upper-shelf toughness regions.^[4–8]

The present study aims to determine and interrelate fracture toughness properties CVN, K_{IC} , J_{IC} , J_{IC} , and CTOD_{IC} for six grades of a high-strength martensitic steel within the hardness range from 270 to 475 HB. A single fracture toughness property may then be used as a geometry-independent fracture criterion for each of the steel grades.

2. Material and Specimens

2.1 Material

The material used was a medium alloy steel designated as 30XH2MØA, according to the Russian specifications (GOST 4543.57), having a chemical composition (wt.%) as follows: 0.3C, 0.46Mn, 0.31Si, 0.021P, 0.011S, 0.79Cr, 2.07Ni, 0.42Mo,

N.M. Abd-Allah, Technical Departments, Maadi Company for Engineering Industry, Cairo, Egypt; M.S. El-Fadaly, Mechanical Production Department, Faculty of Engineering, Suez-Canal University, Egypt; M.M. Megahed, Mechanical Design and Production Department, Faculty of Engineering, Cairo University, Egypt; and A.M. Eleiche, Mechanical Engineering Department, King Fahd University of Petroleum and Minerals, Saudi Arabia. Contact e-mail: eleichea@kfupm.edu.sa.

Table 1 Uniaxial tensile properties of 30XH2MØA martensitic steel at six material conditions^[9]

Steel grade	Tempering temperature, °C	<i>E</i> (GPa)	σ_{ys} (MPa)	True ductility ϵ_f
A1 (270 HB)	650	200	857	0.99
A2 (305 HB)	630	200	1001	0.92
A3 (340 HB)	600	201	1110	0.87
A4 (370 HB)	540	202	1185	0.80
A5 (420 HB)	400	202	1370	0.71
A6 (475 HB)	200	202	1485	0.60

0.07Cu, and 0.26V. The steel was supplied in the forged condition. After being rough machined longitudinally from the delivered stock, specimens were heat treated by austenizing at 850 °C for 15 min and then oil quenched. In order to avoid any aging, immediately after quenching, the specimens were tempered at six different temperatures: 650, 630, 600, 540, 400, and 200 °C for 2 h, and then air cooled to room temperature. This yielded six high-strength martensitic steel grades with hardness values of 270, 305, 340, 370, 420, and 475 HB, designated hereafter by A1, A2, A3, A4, A5, and A6, respectively. Table 1 depicts the uniaxial tensile properties, at room temperature, of these six grades.^[9]

2.2 Specimens

The CVN impact specimen geometry used in the present study was chosen according to the ASTM E23^[2] standard with a cross section $10 \times 10 \text{ mm}^2$. The specimens were semifinished by suitable machining after carrying out the prescribed heat treatment operations. All specimens were then ground properly and accurately to final dimensions, except for the V-notch that was finally machined using a honed carbide form tool. After the final machining operation, all test specimens were examined and inspected to ensure complete compliance to the dimensional tolerances specified in the standard. Figure 1 depicts the standard single-edge notched bend (SENB) specimen,^[10] used in the present study to conduct K_{IC} , J_{IC} , and J_{IC} tests. The specimen had a thickness ($B = 12.5 \text{ mm}$) equal to half the width ($W = 25 \text{ mm}$) and was tested in three-point bending over a span length $S = 4W = 100 \text{ mm}$.

3. Test Method and Data Reduction

3.1 CVN Test

All impact tests were carried out employing a pendulum impact testing machine of 300 J capacity at impact velocity of 5 m/s. The CVN tests were conducted on each of the six steel grades over a wide range of temperatures, from -120 to 60 °C. Below room temperature, the specimens were held in a controlled temperature container filled with liquid alcohol; the specimen was normally cooled in an agitated bath to the desired temperature within 1 °C for 20 min. Above the ambient temperature, the specimens were immersed in agitated oil and held at the desired temperature within 1 °C for 20 min. Following the prespecified cooling or heating, each specimen was carried over

a centering jig to the impact tester and broken within 5 s.^[2] For each of the six steel grades, the transition temperature, T_t , was defined from the CVN test results at the temperature corresponding to 50% of the maximum impact energy, I_{max} .^[11]

3.2 K_{IC} and J_{IC} Tests

Each SENB specimen was attached with knife edges suitable to be in contact with a clip gauge to enable measuring the crack-mouth opening displacement (CMOD). The tests were conducted using a servohydraulic testing machine of 600 KN capacity. The specimen was monotonically loaded in bending to a prescribed displacement level, and the loading rate was chosen such that the rate of change of the stress intensity factor, K , was $1 \text{ MPa}\sqrt{\text{m/s}}$. The applied load, P , load-line displacement, V , and time, t , were recorded continuously and processed via an attached computer. Further, CMOD was plotted versus time using a Y-time plotter.

3.3 Data Reduction in K_{IC} Test

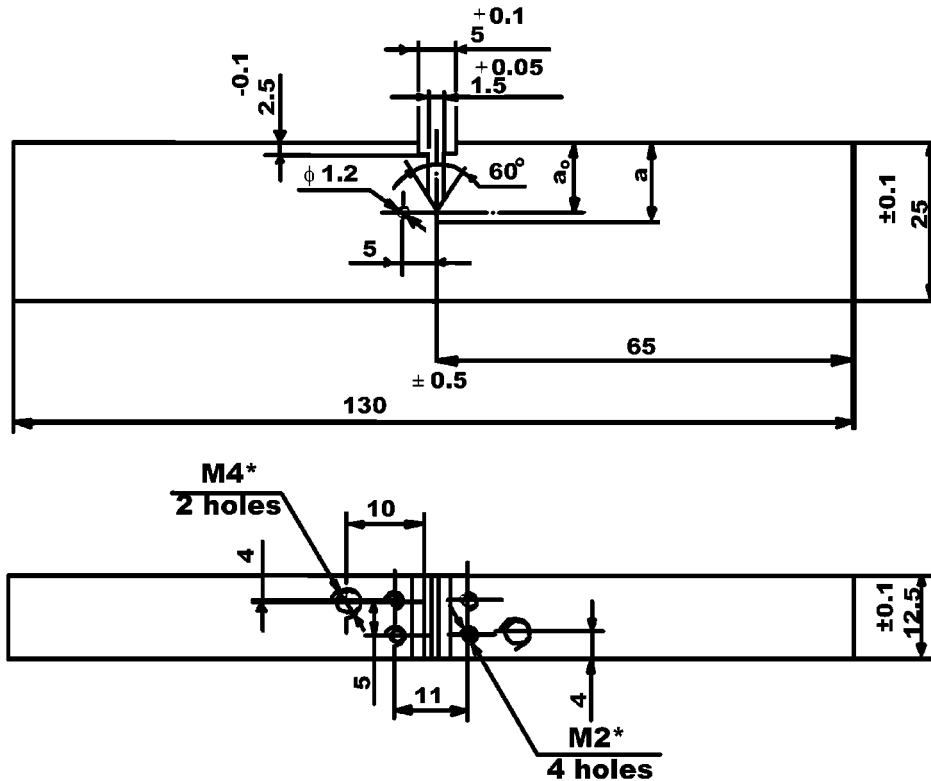
Four specimens of steel grades A5 (420 HB) and A6 (475 HB) were tested according to the conditions of the ASTM E399 standard test method.^[10] Consequently, the candidate fracture toughness K_Q was defined. The average mean value of K_Q for each steel grade was considered to be the plane strain fracture toughness, K_{IC} (i.e., $K_Q = K_{IC}$), since all conditions of ASTM E399 standard test method were satisfied.

3.4 Data Reduction in J_{IC} Tests

A multiple-specimen technique was employed according to the ASTM E813 standard test method.^[12] Five or six identically prepared specimens of each of steel grades A1 (270 HB), A2 (305 HB), A3 (340 HB), and A4 (370 HB) were tested to selected different displacement levels. Thereafter, the crack extension was marked for each specimen, after unloading, by heat tinting at 300 °C for 30 min. The specimen was then broken to expose the crack extension, Δa , which was measured by an optical traveling microscope. The candidate fracture toughness, J_Q , was determined for each steel grade by the intersection point between the corresponding J - Δa curve and an offset line plotted parallel to a blunting line ($J = 2 \sigma_{ys} \Delta a$) at an offset value of 0.2 mm. The value of J_Q was considered equal to J_{IC} on the basis that the test results satisfied the conditions of the ASTM E813 standard test method. During J -integral testing, CMOD was measured for all specimens and the corresponding CTOD (δ) was calculated according to BS 5762.^[13]

3.5 J_{IC} and $CTOD_{IC}$ Tests

The principle of the DCPD method^[4] was utilized for the bend specimen of the present study. A constant direct current was fed into the specimen in the plane of loading, and the potential drop, φ , was measured at two contact pins across the crack. The value of φ changes when the specimen is loaded and, especially, when the crack grows. At onset of stable crack growth, a more distinct change of the shape of the φ - t curve is found, and the further change of φ is proportional to the crack growth.^[7] In this way, critical values of force (P_i), load-line displacement (V_i), and crack-mouth opening displacement ($CMOD_i$) can be defined.



*Machined only for J_{IC} and $CTOD_{IC}$ tests

All dimensions in mm

Test / Dimension	K_{IC} (ASTM E399)	J_{IC} (ASTM E813)	J_{IC} and $CTOD_{IC}$ (DCPD Technique)
a_0	9.75	11.50	11.50
a	12.50	13.75	13.75
a/W	0.50	0.55	0.55

Fig. 1 Fracture toughness test specimen used in K_{IC} , J_{IC} , and J_{IC} testing

3.6 Data Reduction in J_{IC} and $CTOD_{IC}$ Tests

At the point of interest (P_i , V_i , and $CMOD_i$), the material fracture toughness properties J_{IC} and $CTOD_{IC}$ (δ_{IC}) at the onset of slow stable crack growth were determined.

4. Results and Discussion

4.1 CVN Test Results

The results obtained from CVN impact tests at different temperatures are shown separately in Fig. 2. Furthermore, Fig. 3 compares the CVN absorbed energy-temperature curves for the six steel grades. From the variation of impact energy with temperature, the transition temperature, T_t , and the upper shelf

impact energy, I_{max} , were determined for each material condition, as listed in Table 2. The test results indicate that T_t increases with material hardness. The value of T_t was found to be -74 , -60 , -53 , and -45 °C, corresponding to hardness values of 270, 305, 340, and 370 HB, respectively. Consequently, at temperatures higher than -45 °C, 30XH2MØA martensitic steel will exhibit notch-tough behavior within the hardness range of 270 to 370 HB. On the other hand, there is no definite transition temperature from notch-brittle to notch-tough behavior in the hardness range 420 to 475 HB, within the testing temperature zone of the present study. At the testing temperature of 60 °C, examination of the fracture surfaces of the tested specimens of material conditions A5 (420 HB) and A6 (475 HB) indicated 70% granular (cleavage) appearance. Therefore, in the range of hardness higher than 420 HB, the steel is pre-

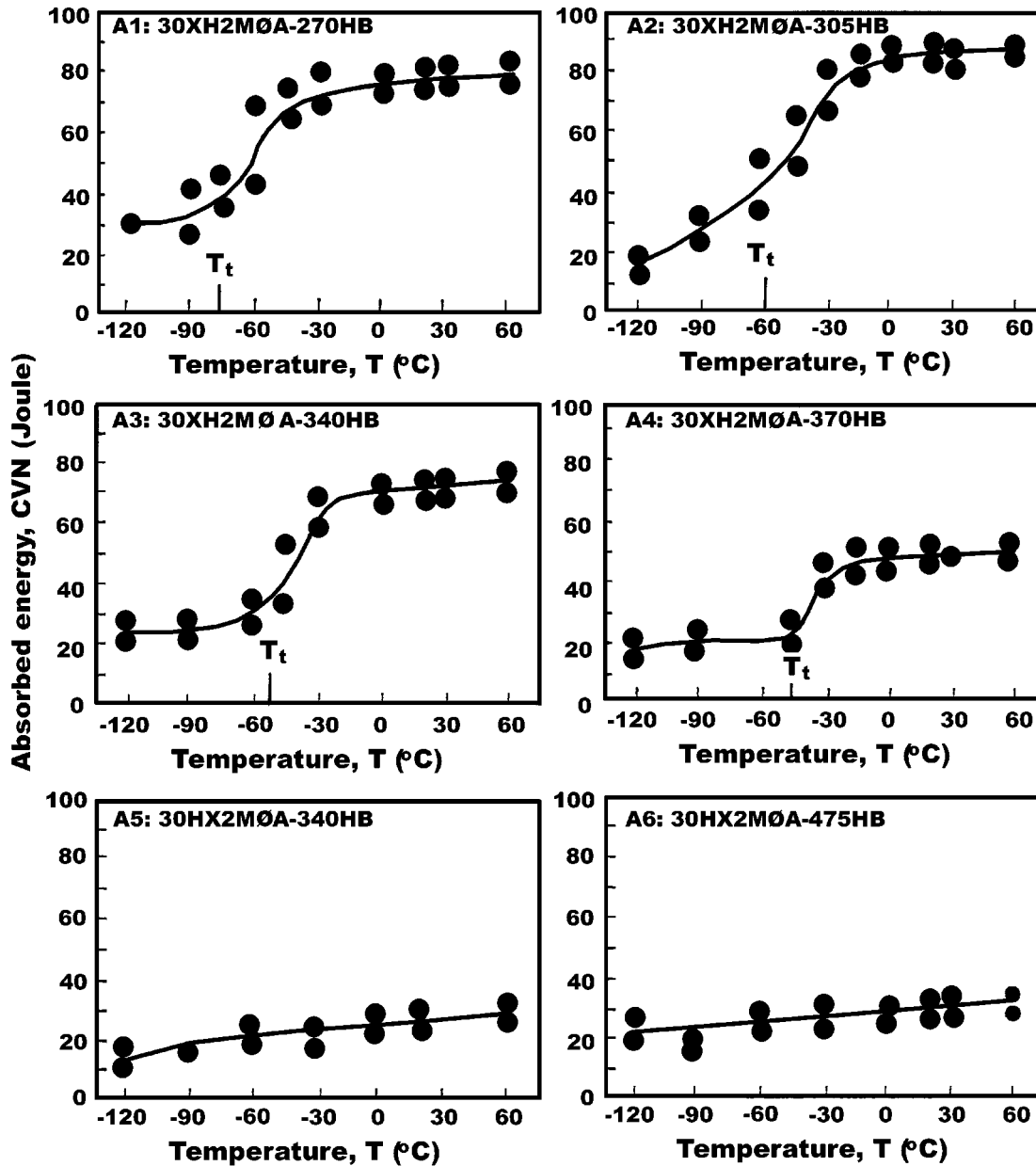


Fig. 2 CVN absorbed energy vs temperature, T , for the six material conditions

dicted to demonstrate notch-brittle behavior when testing at temperatures below 60 °C.^[1]

4.2 Estimation of K_{IC} from CVN Test Results

Plane strain fracture toughness (K_{IC}) can be predicted for metals from their corresponding CVN test results using several empirical relations. At the upper shelf, Rolfe-Novak-Barsom^[14,15] showed that the effect of CVN acuity and loading rate are not so critical as in the transition-temperature region. They indicated that, within the upper shelf, the differences in K_{IC} and CVN test specimens (namely, notch acuity and loading rate) are not significant; a reasonable correlation has been derived experimentally, given by

$$\left(\frac{K_{IC}}{\sigma_{ys}}\right)^2 = \frac{5}{\sigma_{ys}} \left(\text{CVN} - \frac{\sigma_{ys}}{20}\right) \quad (\text{Eq 1})$$

where K_{IC} is in Kpsi $\sqrt{\text{in.}}$, σ_{ys} in Kpsi, and CVN in ft-lb.

Further, Barsom and Rolfe^[1,16] derived another empirical correlation in the transition region, given by

$$\frac{K_{IC}^2}{E} = 2(\text{CVN})^{3/2},$$

$$T_{\text{shift}} = 215 - 1.5 \sigma_{ys} \dots \text{ for } 36 < \sigma_{ys} < 140 \quad (\text{Eq 2})$$

where K_{IC} is in psi $\sqrt{\text{in.}}$, E in psi, CVN in ft-lb, σ_{ys} at room

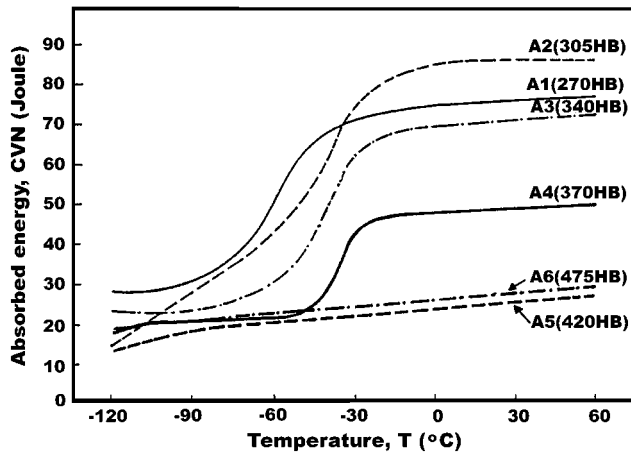


Fig. 3 Representative curves of CVN behavior for all material conditions

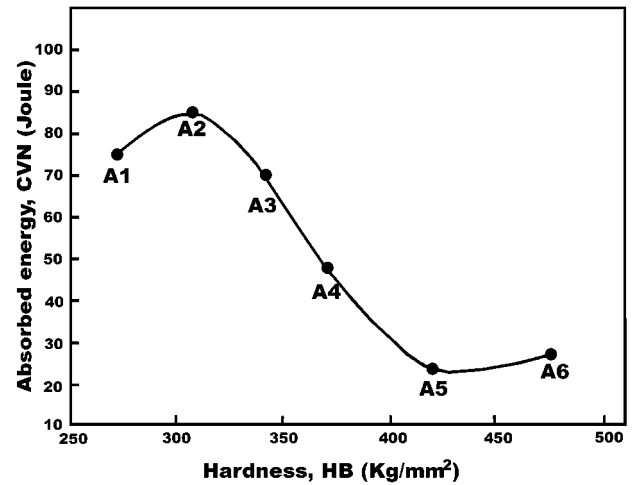


Fig. 4 Charpy impact test results for 30XH2MØA steel at room temperature; A1 through A6 are the various steel grades used (Table 1)

Table 2 Results of CVN impact test for 30XH2MØA steel and the corresponding estimation for K_{IC} test, at 20°C

Steel grade	Upper-shelf impact energy, I_{max} (J)	Transition temperature, T_t (°C)	Estimation for K_{IC} test			
			K_{IC}^* (MPa \sqrt{m})		$B = 2.5 \left(\frac{K_{IC}^*}{\sigma_{ys}} \right)^2$ mm	
			Eq 1	Eq 2	Eq 1	Eq 2
A1 (270 HB)	75	-74	192.0	170.0	125	98
A2 (305 HB)	85	-60	220.5	186.5	121	87
A3 (340 HB)	70	-53	206.0	161.5	86	53
A4 (370 HB)	48	-45	167.0	122.0	50	26
A5 (420 HB)	24	...	96.5	72.5	12	7
A6 (475 HB)	27	...	109.0	79.5	13	7

temperature in psi, and T_{shift} the temperature shift in °F, between slow-bend loading and impact loading in steels. For 30XH2MØA high-strength steel, Eq 2 depicts that T_{shift} can be neglected.

Figures 2 and 3 indicate that, at room temperature, the CVN behavior of steel grades A1, A2, A3, and A4 is within the upper shelf region of each grade, while the behavior of steel grades A5 and A6 is at the transition region. However, the two equations have been utilized in the present paper to predict plane strain fracture toughness, K_{IC}^* , at room temperature for the six steel grades, whether the grade is at the upper shelf or the transition region.

Following Rolfe-Novak-Barsom^[14,15] (Eq 1), and Barsom and Rolfe (Eq 2), Table 2 lists the predicted plane strain fracture toughness values (K_{IC}^*) at room temperature for the six steel grades. The initial selection of a specimen size from which valid values of K_{IC} will be obtained may be based on an estimated value of K_{IC} . Consequently, the estimated thickness, B , for the SENB specimen recommended for use in K_{IC} tests^[10] has been calculated for each steel grade, $B \geq 2.5(K_{IC}^*/\sigma_{ys})^2$, and listed in Table 2. The table indicates that, within a hardness range of 270 to 370 HB, the recommended specimen thickness range for the K_{IC} test is $B = (125 \text{ to } 50 \text{ mm})$, respectively. These specimen sizes are impractical and too large to be used

in K_{IC} tests. Thus, fracture toughness of the steel within the hardness range 270 to 370 HB is recommended to be determined by the integral value according to test method ASTM E813.^[12] Furthermore, the table depicts that the steel within the hardness range 420 to 475 HB may be tested in K_{IC} using relatively small specimen size, $B = 7 \text{ to } 13 \text{ mm}$.

4.3 Variation of CVN Values with Hardness at Room Temperature

Figure 4 depicts the variation of CVN absorbed energy with hardness for the steel at room temperature. The figure shows that there is a minimum in the curve in the region 420 to 475 HB, corresponding to the tempering temperature zone of 400 to 200 °C, respectively. It has been reported^[17,18,19] that this minimum is usually observed in impact testing of martensitic steels, such as 4340 steels,^[20] tempered within the temperature zone of 250 to 400 °C. This phenomenon is most noticeable with tempering temperature of 300 °C,^[18] therefore, it has been called 300 °C embrittlement. The cause is attributed to the retained austenite that changes into temper martensite and the steel expanding in volume since austenite occupies a smaller volume than martensite. Also, the previously existing martensite undergoes a nonuniform transformation. Diffusion proceeds

Table 3 K_{IC} test results

Specimen number	P (N)	A/w	K_Q (MPa \sqrt{m})	$2.5 (K_Q/\sigma_{ys})^2$ (mm)
A5: 30XH2M \varnothing A—420 HB				
A5-1	18,248	0.475	89.96	10.78
A5-2	17,885	0.475	88.19	10.36
A5-3	16,964	0.479	84.79	9.58
A5-4	16,758	0.497	88.87	10.20
A6: 30XH2M \varnothing A—475 HB				
A6-1	16,415	0.516	92.19	9.64
A6-2	17,248	0.500	91.97	9.59
A6-3	17,287	0.493	90.52	9.29

Table 4 Regression line equations and the experimentally determined J_{IC} values

Material designation	Regression line equation:	
	$J = c_1 (\Delta a)^{c_2}$ J in (kJ/m ²); Δa in mm	J_{IC} (kJ/m ²)
A1: 30XH2M \varnothing A—270 HB	$J = 234.8 (\Delta a)^{0.41}$	139.7
A2: 30XH2M \varnothing A—305 HB	$J = 308.6 (\Delta a)^{0.457}$	174.5
A3: 30XH2M \varnothing A—340 HB	$J = 256 (\Delta a)^{0.4}$	151.0
A4: 30XH2M \varnothing A—370 HB	$J = 151.3 (\Delta a)^{0.359}$	90.3

faster at the grain boundaries than in the grain bulk, so cementite is rejected in lamellar form to the boundaries more readily, which is detrimental to the impact resistance of the steel.^[17-19] It is quite clear from the aforementioned discussion that 30XH2M \varnothing A martensitic steel demonstrates a slight 300 °C embrittlement phenomenon. Therefore, the temperature range from 250 to 400 °C should be avoided in assigning tempering temperatures for this steel.

On the other hand, Fig. 4 depicts that 30XH2M \varnothing A martensitic steel is completely free of the defect of temper brittleness, which is usually found in chromium-nickel and chromium-manganese steels when these steels have been slowly cooled after tempering within the temperature zone 425 to 590 °C.^[17-19] This is in agreement with the observations made in the literature^[17-19] that the most radical means of eliminating temper brittleness depends upon alloying a steel with an additional small amount ($\approx 0.4\%$) of molybdenum, which is the case of 30XH2M \varnothing A steel.

At hardness 305 HB, 30XH2M \varnothing A martensitic steel attains the maximum CVN value of 85 J, as shown in Fig. 4. This hardness value of the steel is obtained after tempering the quenched steel at 630 °C. This result is in agreement with observations made in the literature^[15] that the impact value of a steel attains its maximum not after tempering the steel at the A_1 temperature (where $A_1 \approx 723$ °C is the transformation temperature) as is usually believed, but at some lower temperature (600 to 650 °C). This can be explained as follows:^[18] as the tempering temperature of a steel increases, the cementite grains gradually grow (coagulate) resulting in increasing the impact value of the steel. After a certain critical “coarseness” has been reached, the further coarsening of the cementite grains causes a decrease (though small) in the impact value.

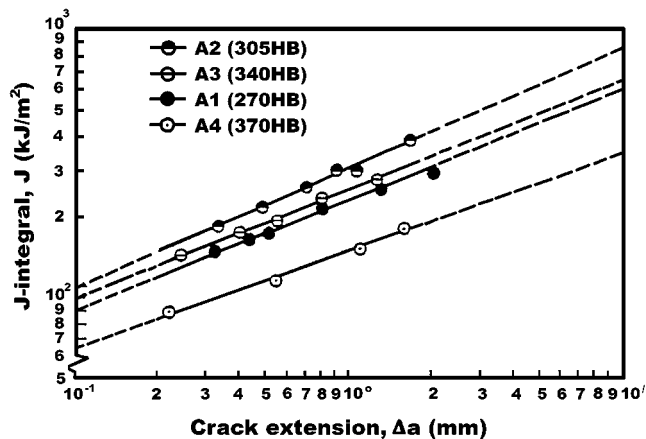


Fig. 5 Logarithmic plot of the J -integral, J , vs crack extension, Δa , for 30XH2M \varnothing A martensitic steel at four material conditions

4.4 K_{IC} Test Results

The candidate fracture toughness, K_Q , for each specimen of the steel was calculated according to a standard test method^[10] and the results are summarized in Table 3. The results indicate that the selected size of the SENB specimen, $B = 12.5$ mm, satisfies the ASTM E399 condition $B \geq 2.5 (K_Q/\sigma_{ys})^2$. This indicates the valid selection of the specimen size based on the CVN test results, as listed in Table 2. All other conditions of the standard test method were checked to be valid. Consequently, the valid determined K_{IC} values are 87.95 and 91.55 MPa \sqrt{m} for steel grades A5 (420 HB) and A6 (475 HB), with root-mean-square errors of 1.93 and 0.75, respectively.

4.5 J_{IC} Test Results

The J -integral values were plotted against Δa , using at least four data points within the prespecified limits of crack extension. Figure 5 depicts a logarithmic plot of the J - Δa responses. Using a least-squares method, the J -integral versus crack growth behavior was determined with a best-fit-power relationship of the form $J = c_1 (\Delta a)^{c_2}$. Table 4 lists the regression line equation and J_{IC} value for each steel grade. The determined J_{IC} values are 139.7, 174.5, 151, and 90.3 kJ/m² for steels at hardness 270, 305, 340, and 370 HB, respectively. The results listed indicate that each of J_{IC} , J -integral coefficient, c_1 , and crack extension exponent, c_2 , attains its maximum value at 305 HB.

Figure 6 depicts the variation of J_{IC} and CVN values with hardness. It is clear that the variation of CVN values is similar to that of J_{IC} values. At a hardness level of 305 HB, J_{IC} attains its maximum value of 174.5 kJ/m², and CVN attains its maximum value of 85 J. Thereafter, both J_{IC} and CVN values decrease as the material hardness deviates from 305 HB. The similarity between the J_{IC} test and CVN test values can be interpreted from the fact that the two types of tests are considered interrelated fracture toughness criteria.^[17]

4.6 J_{IC} and $CTOD_{IC}$ Test Results

The experimentally determined fracture toughness, J_{IC} , is 108, 130.7, 115.5, and 64.2 kJ/m² for steels with hardnesses

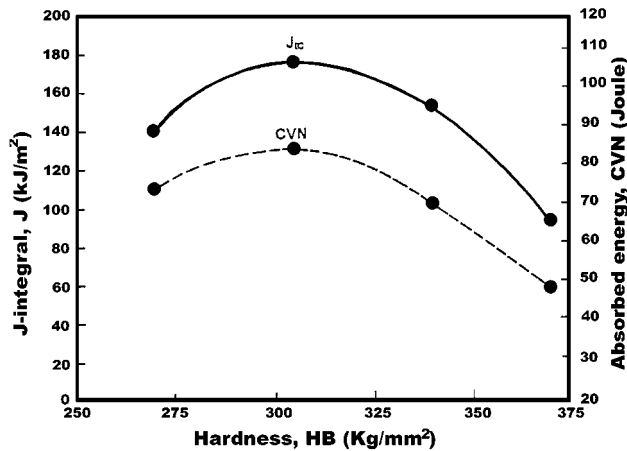


Fig. 6 Variation of J_{IC} and CVN values with hardness for the 30XH2MØA martensitic steel

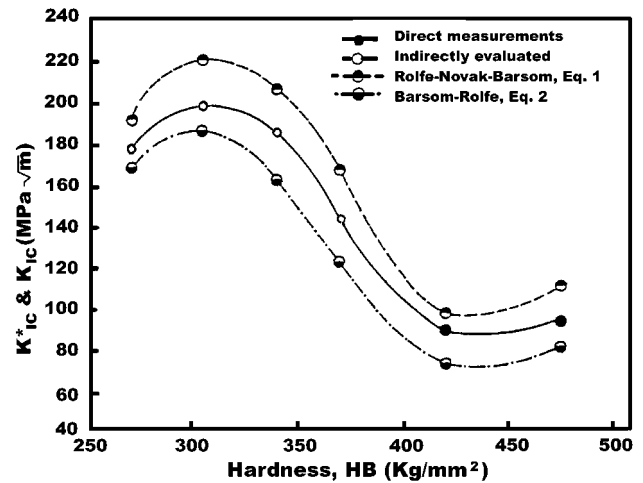


Fig. 7 Measured (directly and indirectly evaluated) and predicted K_{IC} values for 30XH2MØA martensitic steel

Table 5 Fracture toughness properties for 30XH2MØA martensitic steel

Material designation	K_{IC} (MPa√m)	K_o (MPa√m)	J_{IC} (kJ/m ²)	J_{IC} (kJ/m ²)	CTOD _{IC} (mm)
A1: 30XH2MØA—270 HB	177.10	155.7	139.7	108.0	0.090
A2: 30XH2MØA—305 HB	197.90	171.3	174.5	130.7	0.098
A3: 30XH2MØA—340 HB	184.60	161.4	151.0	115.5	0.080
A4: 30XH2MØA—370 HB	143.10	120.6	90.3	64.2	0.041
A5: 30XH2MØA—420 HB	87.95	82.0	34.1	29.7	0.022
A6: 30XH2MØA—475 HB	91.55	86.9	37.0	33.3	0.022

270, 305, 340, and 370 HB, respectively. Further, the crack-tip opening displacement at the onset of crack initiation (CTOD_{IC}) was determined for each steel grade. The corresponding CTOD_{IC} values are 0.09, 0.098, 0.08, and 0.041 mm, respectively. Fracture toughness test results are listed in Table 5, where it is seen that J_{IC} and CTOD_{IC} attain their maximum values at 305 HB.

4.7 Variation of K_{IC} with Hardness

The value of K_{IC} for each of the material conditions A1(270 HB), A2(305 HB), A3(340 HB), and A4(370 HB) was evaluated from its experimentally determined J_{IC} value, as follows:^[21]

$$K_{IC} = \sqrt{EJ_{IC}/(1 - \nu^2)} \quad (\text{Eq } 3)$$

Table 5 depicts that the calculated K_{IC} values are 177.1, 197.9, 184.6, and 143.1 MPa√m for material conditions A1, A2, A3, and A4, respectively. These calculated values together with the directly measured K_{IC} values for steel grades A5 (420 HB) and A6 (475 HB) are plotted versus material hardness in Fig. 7. The figure depicts that the steel attains its maximum K_{IC} value at a hardness value of 305 HB. Thereafter, the K_{IC} value decreases for higher and lower hardnesses. Further, the figure shows that the K_{IC} value at 420 HB is slightly smaller than the one at 475 HB. This indicates the existence of a slight temper brittleness phenomenon within the hardness range 420 to 475 HB, corresponding to tempering temperature range of

400 to 200 °C, respectively. This is the condition of the 300 °C embrittlement phenomenon.^[21]

For comparison, Fig. 7 also shows the predicted values of K_{IC} , which have been estimated from CVN impact test results, as listed in Table 2. It is clear that Eq 1 developed by Rolfe-Novak-Barsom represents an upper bound, while Eq 2 developed by Barsom-Rolfe represents a lower bound, of K_{IC} values for 30XH2MØA martensitic steel within the hardness range of 270 to 475 HB.

4.8 Variation of K_{IC} with Tempering Temperature

Figure 8 depicts the variation of K_{IC} with the tempering temperature, T . The figure shows that the hardened steel acquires its maximum fracture toughness at a tempering temperature of 630 °C, corresponding to a material hardness of 305 HB. Thereafter, K_{IC} decreases almost linearly for higher and lower tempering temperature.

In certain applications of 30XH2MØA martensitic steel, it is highly desirable to maximize fracture toughness and material yield strength.^[22] Tempering the quenched steel at 650, 630, and 600 °C will yield hardness values 270, 305, and 340 HB, corresponding to the three material conditions A1, A2, and A3, respectively. Tables 1 and 4 list σ_{ys} and J_{IC} , respectively, for the three material conditions. A comparison between the considered properties for these material conditions indicates that σ_{ys} and J_{IC} for hardness 270 HB are lower than the corresponding values for 305 and 340 HB by (14.5%, 20%) and (23%, 7.5%),

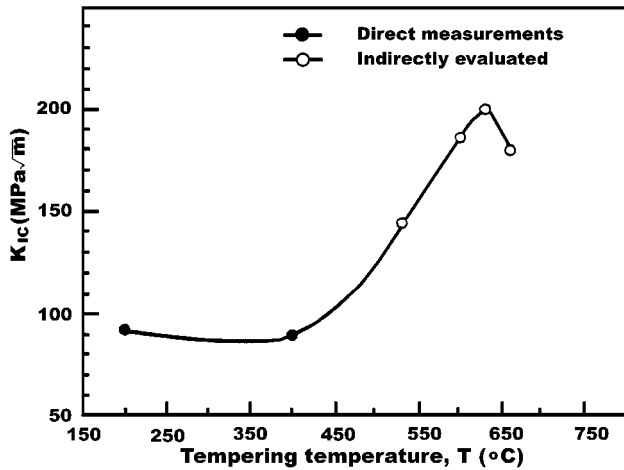


Fig. 8 Directly and indirectly evaluated K_{IC} vs tempering temperature for the 30XH2MØA martensitic steel

respectively. Therefore, J_{IC} test results of the present study indicate the necessity to temper the quenched steel within the temperature zone 600 to 630 °C. Moreover, it is recommended to avoid tempering the quenched 30XH2MØA steel at temperatures higher than 630 °C.

Adjusting the tempering temperature at 400 and 200 °C will yield hardness values 420 and 475 HB, corresponding to material conditions A5 and A6, respectively. Tables 1 and 3 indicate that σ_{ys} and K_{IC} for material A5 are lower than the corresponding values for material A6 by 7.7 and 3.9%, respectively. Therefore, K_{IC} test results indicate the necessity to temper the quenched steel at 200 °C instead of 400 °C. This will optimize fracture toughness and tension properties of the steel and avoid the condition of 300 °C embrittlement usually occurring during tempering martensitic alloy steels within the temperature range 250 to 400 °C.^[17]

4.9 Variation of K_o , K_{IC} , J_{IC} , and $CTOD_{IC}$ with Hardness

Several investigators argued that satisfying ASTM E399 conditions of specimen thickness does not ensure the determination of true plane strain fracture toughness, K_o .^[21] This has been verified by experimental tests that indicated that K_o is obtained at the onset of crack initiation.^[21] The fracture toughness, K_o , has been found to be independent of specimen thickness and to have a constant value for a particular material. True plane strain fracture toughness, K_o , has been evaluated for the six steel grades as follows. For material conditions A5 (420 HB) and A6 (475 HB), K_o has been computed from their experimentally determined K_{IC} values and monotonic tension properties as follows:^[23]

$$K_o = K_{IC} / \sqrt{1 + \frac{\epsilon_f E}{24 \sigma_{ys}} \cdot \frac{B_o}{B}} \quad (\text{Eq 4})$$

where ϵ_f , E , and σ_{ys} are the true fracture ductility, elastic modulus, and yield strength of the considered material; $B_o = K_{IC}^2 / (3 \pi \cdot \sigma_{ys}^2)$ = plastic zone size in plane strain; and B = actual specimen thickness in standardized K_{IC} test. Thus,

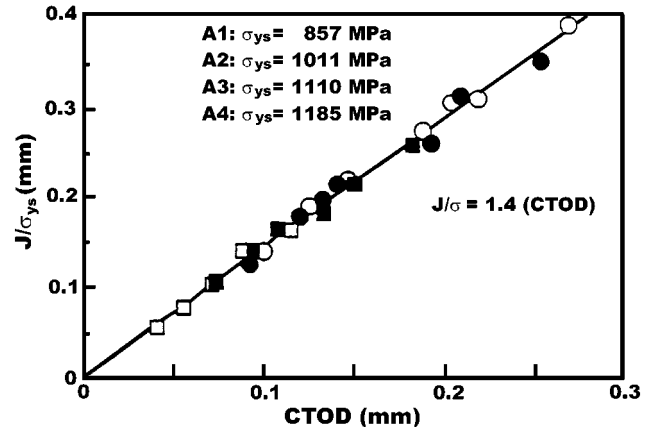


Fig. 9 Variation of J/σ_{ys} with CTOD for 30XH2MØA martensitic steel within the σ_{ys} range of 857 to 1185 MPa

the corresponding K_o values are 82 and 86.9 MPa \sqrt{m} respectively. Further, values of K_o can be calculated from the experimentally measured J_{IC} value as follows. Replacing J_{IC} and K_{IC} by J_{IC} and K_o , Eq 3 can be rewritten as

$$K_o = \sqrt{E J_{IC} / (1 - \nu^2)} \quad (\text{Eq 5})$$

where ν is Poisson's ratio. The calculated K_o values are 155.7, 171.3, 161.4, and 120.6 MPa \sqrt{m} for material conditions A1 (270 HB), A2 (305 HB), A3 (340 HB), and A4 (370 HB), respectively. Replacing J_{IC} by σ_{ys} (CTOD_{IC}), Eq 5 can be rearranged as follows:

$$CTOD_{IC} = \frac{K_o^2 (1 - \nu^2)}{E \sigma_{ys}} \quad (\text{Eq 6})$$

Table 5 lists all the fracture toughness properties K_{IC} , K_o , J_{IC} , and $CTOD_{IC}$ determined in the present work within the 270 to 475 HB hardness range. The table depicts J_{IC} , J_{IC} , and $CTOD_{IC}$ values for the steel with hardness values 420 and 475 HB. These values were computed using Eq 5 and 6, respectively.

A number of expressions are found in the literature that relate the experimentally derived J values of the tested metal with the corresponding computed CTOD over the full range of loading. They all take the following linear form: $J = m \cdot \sigma_{ys} \cdot (CTOD)$, where m is a dimensionless factor ranging from 0.7 to 3.0 and depends on the constraining condition and the tested material.^[24,25] Utilizing the J_{IC} and J_{IC} test results listed in Table 5, the values of J/σ_{ys} versus CTOD are plotted in Fig. 9, where σ_{ys} is the corresponding material yield strength listed in Table 1. The figure indicates the existence of linearity between J/σ_{ys} and CTOD. A best-fit linear relation was determined as

$$J = 1.4 \sigma_{ys} (CTOD) \quad (\text{Eq 7})$$

where J is in kJ/m², σ_{ys} is in MPa, and CTOD is in mm, which indicates that $m = 1.4$ for 30XH2MØA martensitic steel within the hardness range 270 to 370 HB.

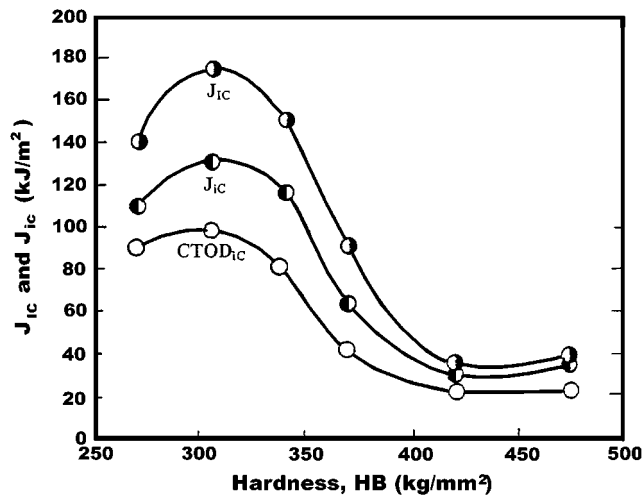


Fig. 10 Variation of J_{IC} , J_{IC} , and $CTOD_{IC}$ with hardness for 30XH2MØA martensitic steel

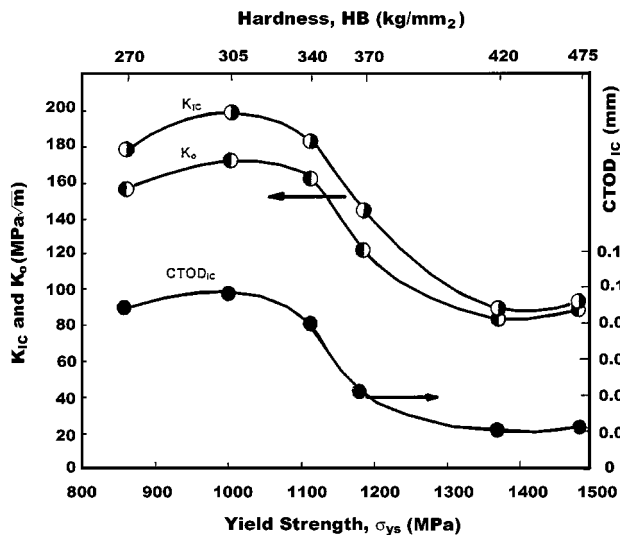


Fig. 11 Variation of K_{IC} , K_o , and $CTOD_{IC}$ with yield strength and hardness for 30XH2MØA martensitic steel

Referring to the fracture toughness properties listed in Table 5, the values of J_{IC} , J_{IC} , and $CTOD_{IC}$ are plotted versus hardness in Fig. 10. Further, Fig. 11 depicts the variation of K_{IC} , K_o , and $CTOD_{IC}$, with σ_{ys} within the hardness range 270 to 475 HB. The figures indicate that all the fracture toughness properties J_{IC} , J_{IC} , $CTOD_{IC}$, K_{IC} , and K_o attain their maximum values at 305 HB. Between 305 and 420 HB, the $CTOD_{IC}$ decreases with the increase in the yield strength and hardness. On the other hand, for hardness values lower than 305 HB and higher than 420 HB, the $CTOD_{IC}$ is almost constant at about 0.094 and 0.022 mm, respectively.

5. Conclusions

1. The transition temperature (T_i) has been determined for 30XH2MØA martensitic steel grades A1 (270 HB), A2 (305

HB), A3 (340 HB), and A4 (370 HB) and found to be -74 , -60 , -53 , and -45 °C, respectively. On the other hand, there is no definite T_i from notch-brittle to notch-tough behavior of martensitic steel grades A5 (420 HB) and A6 (475 HB) within the testing zone of -120 to 60 °C.

2. At room temperature, the martensitic steel of hardness 305 HB, corresponding to tempering at 630 °C, attains its maximum CVN value of 85 J; thereafter, the CVN value decreases with an increase or decrease of material hardness. Further, within the hardness range of 420 to 475 HB corresponding to the tempering temperature zone 400 to 200 °C, 30XH2MØA martensitic steel demonstrates a slight 300 °C temper embrittlement phenomenon, usually observed in the impact testing of martensitic steels.
3. Upper-shelf and transition CVN values of the martensitic steel grades at room temperature have been utilized to estimate successfully the corresponding initial selected size of the specimen intended to be used in K_{IC} testing for martensitic steel.
4. Fracture toughness, K_{IC} , and tension test results of the 30XH2MØA martensitic steel within the hardness range 420 to 475 HB, corresponding to the tempering temperature zone 400 to 200 °C, respectively, optimize the fracture toughness and yield strength at 475 HB.
5. Fracture toughness, J_{IC} and J_{IC} , and tensile properties indicate that the steel acquires the optimum fracture toughness and yield strength condition within the hardness range 305 to 340 HB, corresponding to the tempering temperature zone 630 to 600 °C, respectively.
6. A linear relation has been obtained between the experimentally determined J -integral and $CTOD$ values of the steel within the hardness range 270 to 370 HB.
7. Fracture toughness properties CVN, K_{IC} , K_o , J_{IC} , J_{IC} , and $CTOD_{IC}$, of the steel have been interrelated over the entire hardness range 270 to 475 HB, such that a single fracture toughness property can be used as a geometry-independent fracture criterion.

Acknowledgment

A.M. Eleiche acknowledges the support of KFUPM in the preparation of this paper.

References

1. S.T. Rolfe and J.M. Barsom: *Fracture and Fatigue Control in Structures: Application of Fracture Mechanics*, Prentice-Hall, Englewood Cliffs, NJ, 1987.
2. "Standard Methods for Notched Bar Impact Testing of Metallic Materials," ASTM Standard E23, ASTM, Philadelphia, PA, 1978.
3. S.T. Rolfe, W.A. Sorem, and G.W. Wellman: *J. Constr. Steel Res.*, 1989, vol. 12, pp. 171-95.
4. F.Z. Li, C.F. Shih, and A. Needleman: *Eng. Fract. Mech.*, 1985, vol. 21, pp. 405-21.
5. T.L. Anderson: *Int. J. Fract.*, 1989, vol. 41, pp. 79-104.
6. S.K. Putatunda, J.M. Rigsbee, and H.T. Corten: *JTEVA*, 1985, vol. 13, pp. 181-90.
7. T. Hollstein, J.G. Blauel, and B. Voss: ASTM STP856, ASTM, Philadelphia, PA, 1984, pp. 104-16.
8. P. Hornet and C. Eripret: *Fatigue Fract. Eng. Mater. Struct.*, 1985, vol. 18, pp. 679-92.
9. N.M. Abd-Allah: Ph.D. Dissertation, University of Cairo, Cairo, 1996.

10. "Standard Test Method for Plane-Strain Fracture Toughness of Metallic Materials," ASTM Standard E399-90, ASTM, Philadelphia, PA, 1994.
11. German Standards Organization: "Materialprufnormen fur Metal," Werkstoffe, DIN Taschenbauch 19, Beuth Verlag, Berlin, Koln, DIN 50 115, 1981.
12. "Standard Test Method for J_{IC} , a Measure of Fracture Toughness," ASTM Standard E813-91, ASTM, Philadelphia, PA, 1984.
13. British Standards: "Methods of δ_C , Critical Value of Crack Opening Displacement Testings," British Standard 5762, 1979.
14. S.T. Rolfe and S.R. Novak: "Review of Developments in Plane Strain Fracture-Toughness Testing," ASTM STP 463, Philadelphia, PA, 1970, pp. 124-59.
15. J.M. Barsom and S.T. Rolfe: "Impact Testing of Metals," ASTM STP 466, ASTM, Philadelphia, PA, 1970, pp. 281-302.
16. J.M. Barsom and S.T. Rolfe: *Eng. Fract. Mech.*, 1971, vol. 2, p. 341.
17. G.E. Dieter: *Mechanical Metallurgy*, McGraw-Hill, New York, NY, 1988.
18. V.M. Zuyev: *A Laboratory Manual for Trainees in Heat Treatment*, Mir Publishers, Moscow, 1985.
19. B. Zakharov: *Heat Treatment of Metals*, Moscow, Peace Publishers, Moscow, 1962.
20. S.L. Hoyt: *ASME Handbook*, McGraw-Hill, New York, NY, 1954.
21. D. Broek: *The Practical Use of Fracture Mechanics*, Kluwer Academic Publishers, The Netherlands, 1989.
22. J.W. Ryan: *Guns, Mortars and Rockets*, A. Wheaton & Co. Ltd., Exeter, 1982.
23. D. Broek and H. Vlieger: National Aerospace Institute Report No. 74032, National Aerospace Institute, Amsterdam, 1974.
24. S.K. Putatunda: *JTEVA*, 1986, vol. 14, pp. 49-57.
25. S.A. Paranjpe and S. Banerjee: *Eng. Fract. Mech.*, 1979, vol. 11, pp. 43-53.